

## RELATIONSHIP BETWEEN CAPILLARY PRESSURE AND RESISTIVITY INDEX

Kewen Li\*, Stanford University and Yangtz University and  
Wade Williams, Core Lab, Inc.

\* Corresponding author

*This paper was prepared for presentation at the International Symposium of the Society of Core Analysts held in Toronto, Canada, 21-25 August 2005*

### Abstract

A model has been derived theoretically to correlate capillary pressure and resistivity index. The model is simple and predicts a power law relationship between capillary pressure and resistivity index on a log-log plot. To verify the model, gas-water capillary pressure and resistivity were measured simultaneously at a room temperature in 14 core samples from two formations in an oil reservoir. The permeability of the core samples ranged from 0.028 to over 3000 md. The porosity ranged from less than 8% to over 30%. Capillary pressure curves were measured using a semi-permeable porous-plate technique. The model was tested against the experimental data obtained in this study. The results demonstrated that the model could match the experimental data satisfactorily. Using the model, capillary pressure may be inferred from resistivity data. An existing model was also tested against the experimental data. The results showed that the existing model did not work in most of the cases studied. The new model developed in this study may be useful to evaluate capillary pressure function from resistivity data both in laboratories and reservoirs, especially in the case in which permeability is low.

### Introduction

Both capillary pressure and resistivity index are important parameters in reservoir engineering. It is easier to measure resistivity index than capillary pressure in a laboratory, especially for core samples with low permeabilities. One can run resistivity well logging in a well, even in real time, but cannot do this for capillary pressure. It would be useful if a relationship between capillary pressure and resistivity can be found.

Resistivity, capillary pressure, and relative permeability have similar features. For example, all are a function of fluid saturation in a porous medium and are influenced by pore structure and heterogeneity. Li and Horne<sup>1</sup> derived a model to infer relative permeability from resistivity index. We speculated that capillary pressure may also be derived from resistivity index.

Szabo<sup>2</sup> proposed a linear model to correlate capillary pressure with resistivity by assuming the exponent of the relationship between capillary pressure and water saturation is equal to that of the relationship between resistivity and water saturation. This assumption may not be reasonable in many cases. The linear model proposed by Szabo<sup>2</sup> can be expressed as follows:

$$\frac{R_t}{R_0} = a + bP_c \quad (1)$$

where  $R_0$  is the resistivity at a water saturation of 100%,  $R_t$  is the resistivity at a specific water saturation of  $S_w$ ,  $P_c$  is the capillary pressure,  $a$  and  $b$  are two constants.

The results from Szabo<sup>2</sup> demonstrated that a single straight line, as predicted by the model (Eq. 1), could not be obtained for the relationship between capillary pressure and resistivity index.

Longeron *et al.*<sup>3</sup> measured the resistivity index and capillary pressure under reservoir conditions simultaneously. Longeron *et al.*<sup>3</sup> didn't attempt to correlate the two parameters.

Literature on the relationship between capillary pressure and resistivity index has been scarce. In this study, a theoretical relationship between capillary pressure and resistivity index was derived. In order to verify the relationship, gas-water capillary pressure and resistivity were measured simultaneously in 14 core samples at a room temperature using a semiporous-plate approach.

## Theoretical Background

A theoretical relationship between capillary pressure and resistivity index is derived in this section. The basic idea behind this is that both capillary pressure and resistivity index are a function of the wetting phase saturation and the functions are known from the fractal modeling of a porous medium and are discussed in the following.

Toledo *et al.*<sup>4</sup> reported that resistivity obeys the scaling law at low wetting phase saturations:

$$\frac{1}{R_t} \propto (S_w)^{\frac{1}{\beta(3-D_f)}} \quad (2)$$

where  $\beta$  is the exponent in the relation of disjoining pressures and film thickness,  $S_w$  is the wetting phase saturation, and  $D_f$  is the fractal dimension of the surface of the grains in matrix.

Toledo *et al.*<sup>4</sup> also reported that capillary pressure follows the scaling law at low wetting phase saturations:

$$S_w \propto (P_c)^{-(3-D_f)} \quad (3)$$

Combining Eqs. 2 and 3, one can obtain:

$$P_c \propto (R_t)^\beta \quad (4)$$

It is known that  $R_t$  is equal to  $R_o$  when  $P_c$  is equal to  $p_e$  at a water saturation of 100%, which can be expressed as follows using Eq. 4:

$$p_e \propto (R_o)^\beta \quad (5)$$

Combining Eqs. 4 and 5:

$$P_c = p_e \left( \frac{R_t}{R_o} \right)^\beta \quad (6)$$

Using the dimensionless form, Eq. 6 can be expressed as follows:

$$P_{cD} = (I)^\beta \quad (7)$$

Where  $P_{cD}$  is the dimensionless capillary pressure ( $P_c/p_e$ );  $I$  is the resistivity index and, as a function of the wetting phase saturation, can be represented using the Archie's equation<sup>5</sup>:

$$I = \frac{R_t}{R_o} = S_w^{-n} \quad (8)$$

here  $n$  is the saturation exponent.  $R_o$  depends on the porosity of a porous medium and can be calculated:

$$F_R = \frac{R_o}{R_w} = \phi^{-m} \quad (9)$$

Where  $R_w$  is the resistivity of water,  $m$  is the cementation exponent, and  $F_R$  the formation factor.

According to Eq. 7, dimensionless capillary pressure can be inferred from the resistivity well logging data once the value of  $\beta$  is known. This may provide a new approach to obtain capillary pressure data for reservoir engineering.

## **Experiments**

Experiments were conducted at a room temperature to measure gas-water capillary pressure and resistivity simultaneously. The apparatus, rock and fluid properties are described in this section.

### **Rock and Fluid Properties**

The properties of the core samples used in this study are listed in Table 1. All the core samples were obtained from one oil reservoir. Group 1 core samples were from one formation with a high permeability and Group 2 were from another formation with a low permeability. The permeability in Group 1 ranged from 437 to 3680 md; the permeability in Group 2 ranged from 0.028 to 387 md.

The brine used for Group 1 core samples had a salinity of 90,000 ppm with a resistivity of 0.078 ohm-m at 25°C. The brine used for Group 2 core samples had a salinity of 20,000 ppm with a resistivity of 0.308 ohm-m at 25°C.

### **Apparatus**

The schematic of the apparatus used for the combined measurements of gas-water capillary pressure and resistivity is shown in Fig. 1. The outside diameter of each porous plate was painted with silver paint. The resistivity meter was manufactured by Quad Tech and the model was 1730 LCR. The frequency used in this study was 20,000 hz.

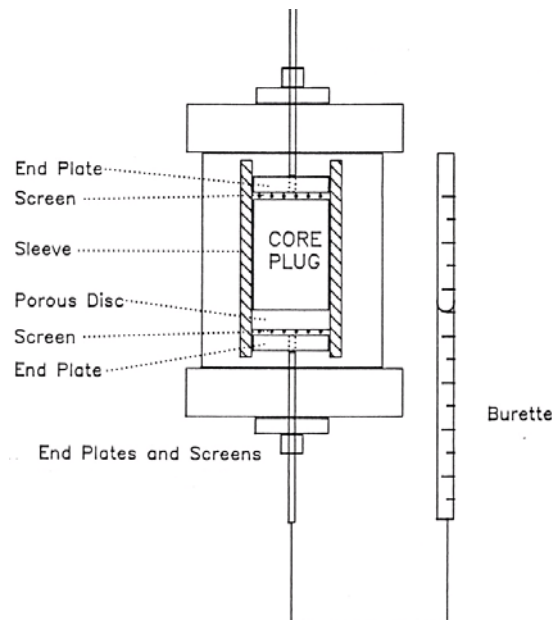


**Fig. 1: Schematic of experimental apparatus for measuring capillary pressure**

### **Experimental Procedure**

The samples designated for these analyses were cleaned and dried prior to testing. Permeability and porosity were measured after cleaning. Then the samples were evacuated and saturated with synthetic formation brine. After loading the sample and the

porous plate into the core holder at an appropriate net stress, brine was flushed using a 500 psi back pressure to ensure a complete saturation. Resistivity was measured, followed by injection of several pore volumes of brine. The resistivity at a water saturation of 100% was measured again the following day until stabilized (less than 1% change per day). Formation resistivity factor (FRF) at stress was determined at this point.

The sample was desaturated beginning at a low pressure by injecting humidified air at a regulated capillary pressure. The volume and weight of displaced brine were monitored and used to calculate the brine saturation. Resistivity, capillary pressure, and brine saturation were measured daily at each pressure point until saturation was stabilized (less than 1% change per day). This was repeated until no water was produced.

At the end of the test, each sample was removed and its weight out was measured. It was Dean-Stark extracted for water, methanol soxhlet extracted for salts, and dried to a constant weight in a vacuum oven at 100°C. The final dry weight was measured. Dean-Stark water extracted was used to confirm the final water saturation.

## Results

The experimental data of capillary pressure and resistivity index in core samples from two formations in one oil reservoir were used to test the model (Eq. 6) proposed in this study. The results are presented and discussed in this section.

Fig. 2 shows the relationship between formation factor and porosity for all the samples from two formations. The values of cement exponent were calculated using Eq. 9:  $m$  is equal to 1.71 for the core samples in Group 1 (formation 1) and is equal to 2.19 for core samples in Group 2 (formation 2).

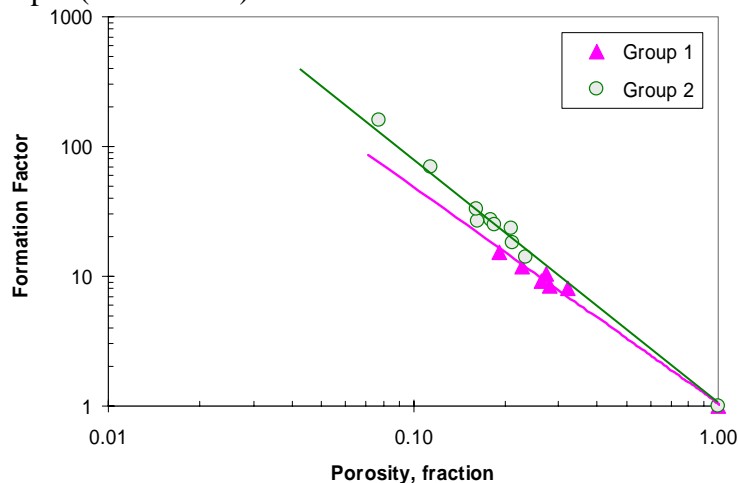


**Fig. 2: Relationship between formation factor and porosity for all the samples from two formations**

The data of resistivity index vs. water saturation for the core samples in Group 1 (high permeability) are shown in Fig. 3. The data points follow the Archie's saturation equation (Eq. 8). The values of saturation exponent were calculated for each core sample using Eq. 8 and the results are shown in Table 1. The value of  $n$  ranges from 1.82 to 2.11 and the

average value is about 1.94. The average value was calculated by conducting regression analysis for all of the data points.

For the low permeability formation (Group 2), the experimental data of resistivity index are shown in Fig. 4. The values of saturation exponent calculated using Eq. 8 are also listed in Table 1. The value of  $n$  ranges from 1.82 to 2.49 and the average value is about 2.13.

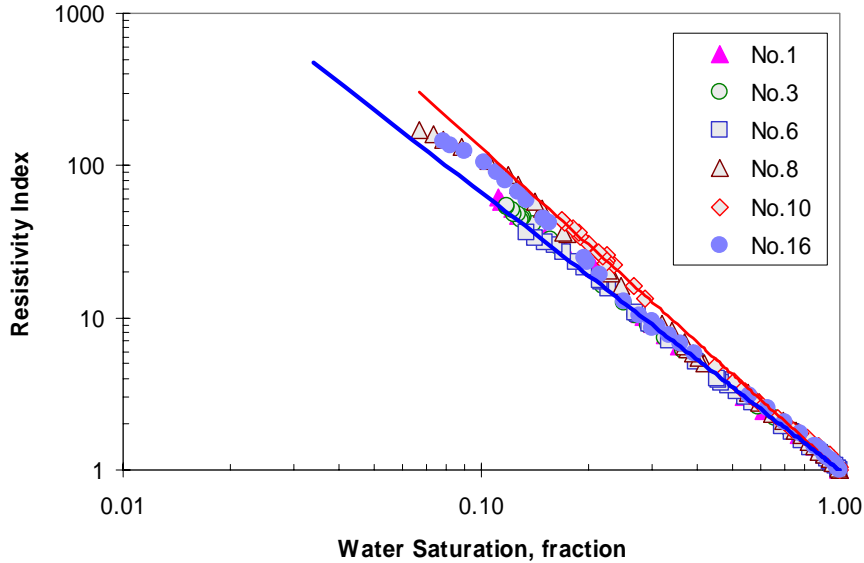


Fig. 3: Relationship between resistivity index and water saturation for the samples in Group 1

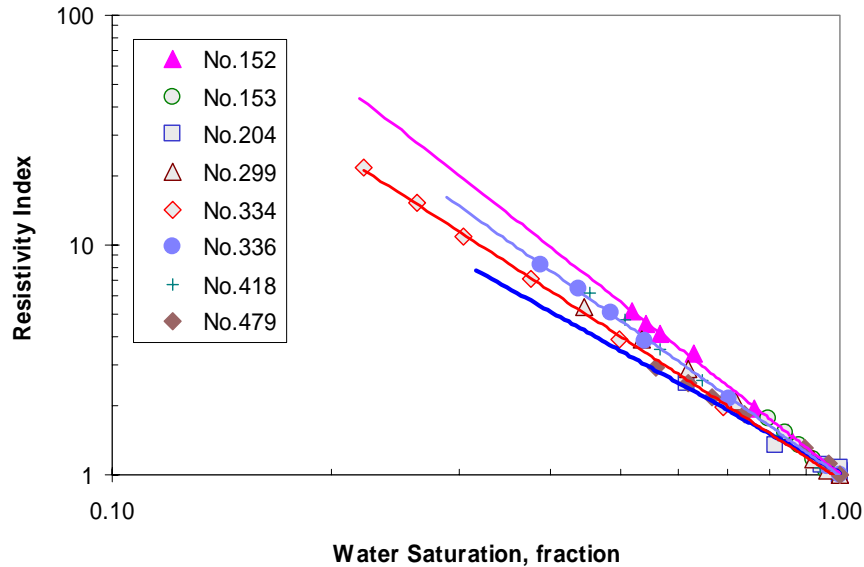


Fig. 4: Relationship between resistivity index and water saturation for the samples in Group 2

It is necessary to have the experimental data of capillary pressure to verify the model represented by Eq. 6. The capillary pressure data of the core samples in Group 1 are shown in Fig. 5 and those of Group 2 are shown in Fig. 6. According to Eq. 3, the relationship between capillary pressure and water saturation is linear in the range of small water saturation. Figs. 5 and 6 show such a feature. Note that the range of water

saturation in which the linear relationship exists is very narrow for the No.3 core sample (see Fig. 5). One can see from Figs. 5 and 6 that the range of water saturation in which the linear relationship exists depends upon permeability. For the core samples with a low permeability, the straight line crosses over almost the entire range of water saturation from 1 to  $S_{wr}$  (residual water saturation). For the core samples with a high permeability, however, the straight line crosses over only the part with small water saturation.

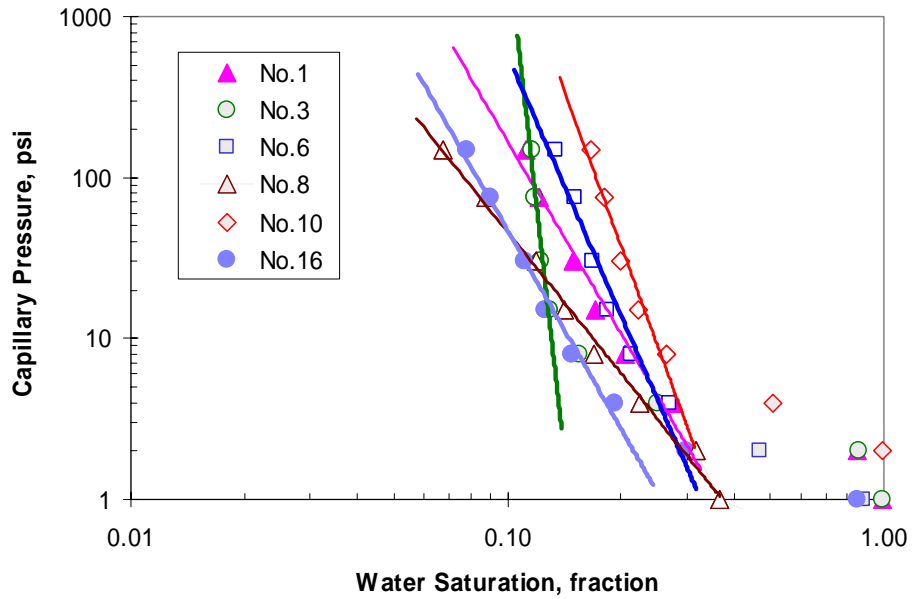


Fig. 5: Capillary pressure curves of the samples in Group 1 (high permeability)

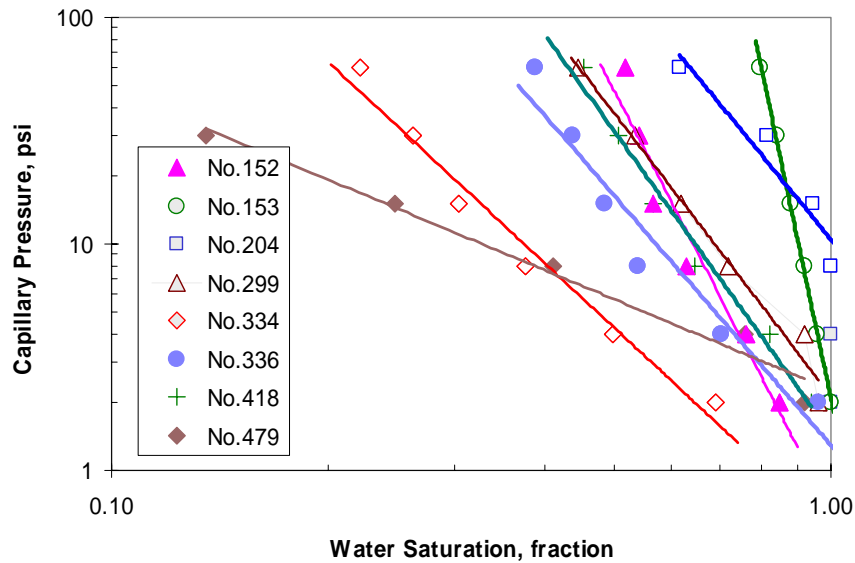


Fig. 6: Capillary pressure curves of the samples in Group 2 (low permeability)

The relationships between capillary pressure and resistivity index of Groups 1 and 2 are shown in Figs. 7 and 8 respectively. In Fig. 7, a straight line exists in the range with great capillary pressure and resistivity index (corresponding to small water saturation), as predicted by the model (Eq. 6) derived in this study.

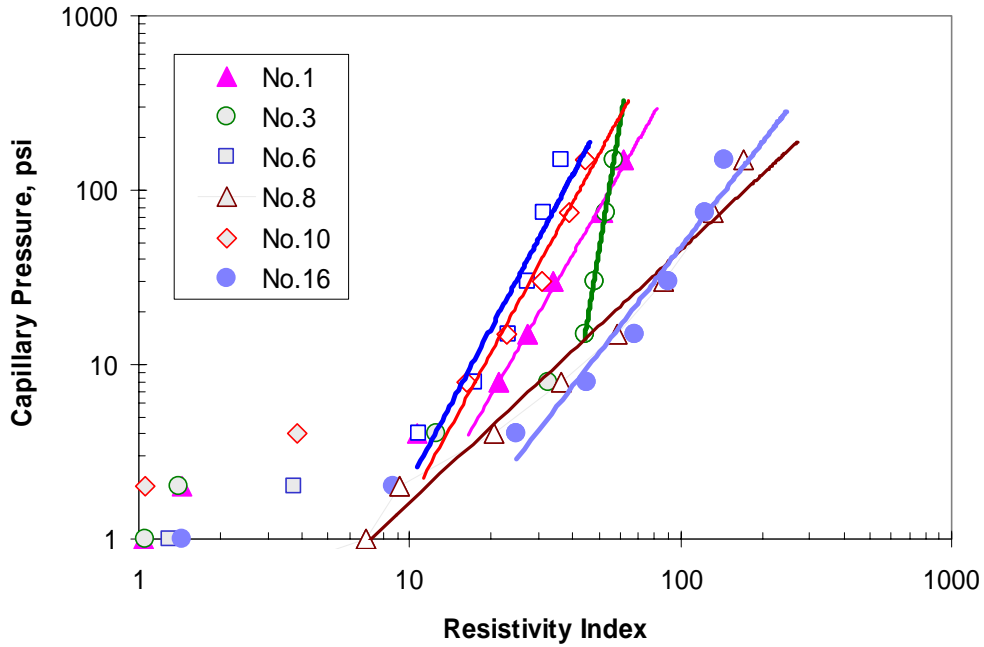


Fig. 7: Relationship between capillary pressure and resistivity index of Group 1 (high permeability)

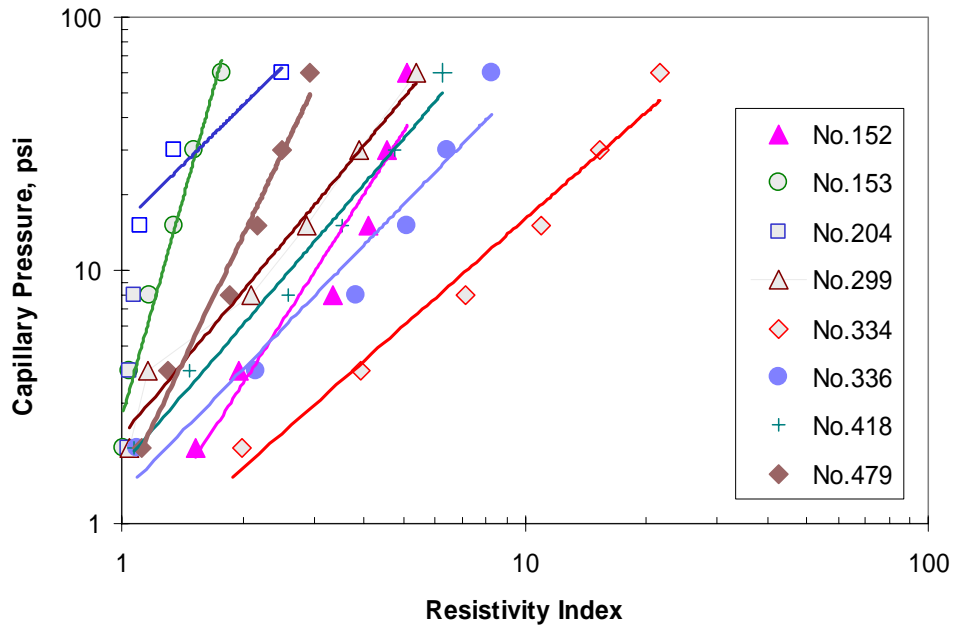


Fig. 8: Relationship between capillary pressure and resistivity index of Group 2 (low permeability)



Interestingly a straight line exists for almost all of the data points in the core samples with a low permeability (see Fig. 8). This demonstrates that the model (Eq. 6) derived from fractal modeling of a porous medium work satisfactorily.

The values of regression coefficient ( $R$ ), i.e., the goodness of fitting, of the model to the data shown in Figs. 7 and 8 were calculated and are listed in Table 1. One can see that the goodness of fitting is satisfactory.

As stated previously, Szabo<sup>2</sup> proposed a linear model (Eq. 1) to correlate capillary pressure and resistivity by assuming the exponent of capillary pressure curve is equal to that of the resistivity index curve. To test this model, the experimental data in Figs. 7 and 8 are plotted in Figs. 9 and 10 using a linear scale instead of a logarithmic scale. Comparing the results shown in Figs. 7 and 8 to those plotted in Figs. 9 and 10, one can see clearly that the model (Eq. 6) derived in this study has a better fitting to the experimental data than the linear model (Eq. 1) in the cases studied.

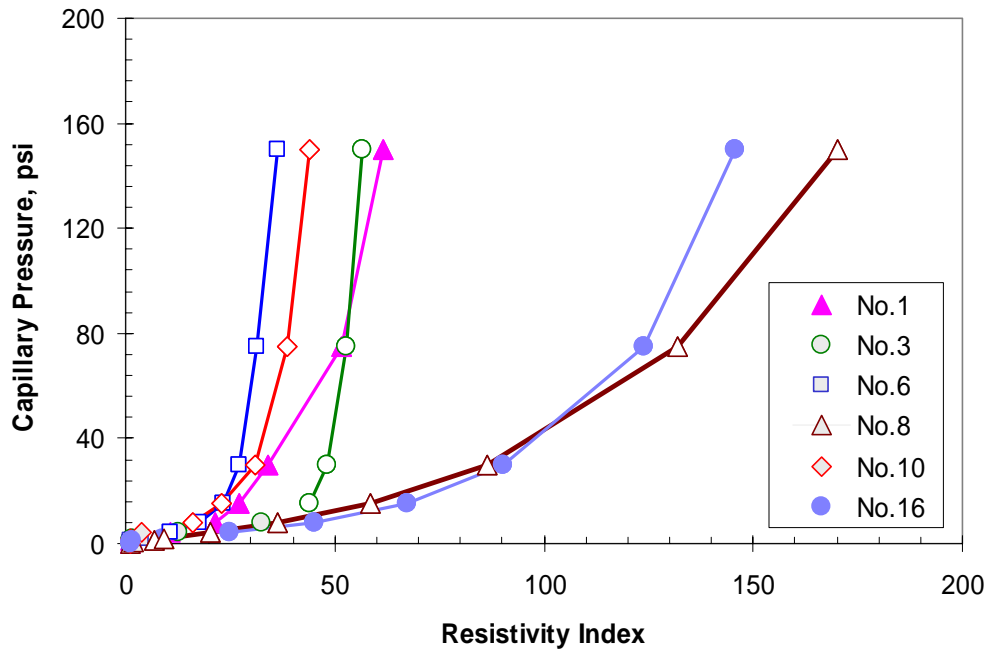


**Fig. 9: Relationship between capillary pressure and resistivity index of Group 1 (high permeability) in a linear coordinate plot**

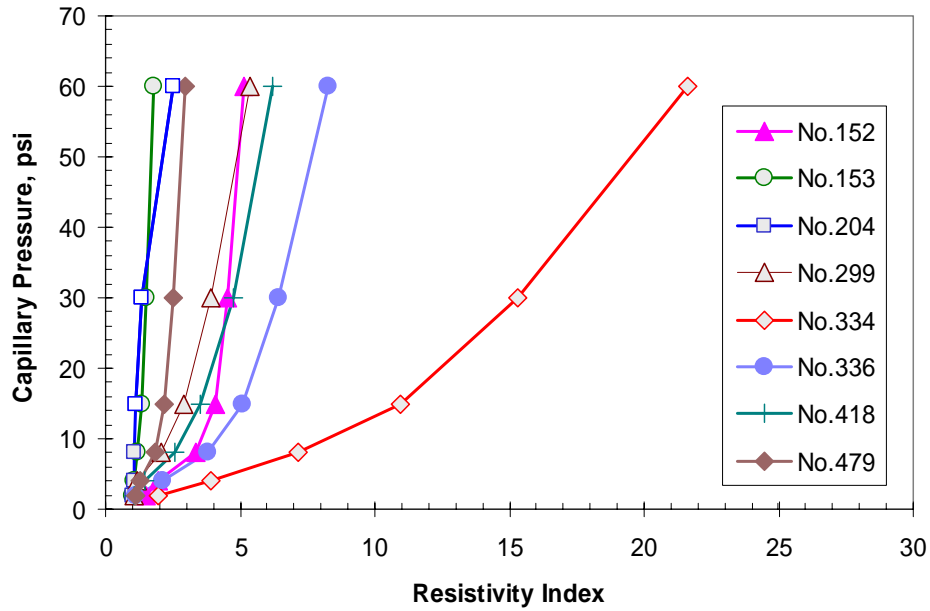


**Fig. 10: Relationship between capillary pressure and resistivity index of Group 2 (low permeability in a linear coordinate plot)**

The values of  $\beta$  were calculated using Eq. 6 with the data shown in Figs. 7 and 8. For most of the core samples, the value of  $\beta$  is in the range from 1 to 3. The effect of permeability on  $\beta$  for the core samples in both Group 1 and 2 is shown in Figs. 11 and 12 respectively.

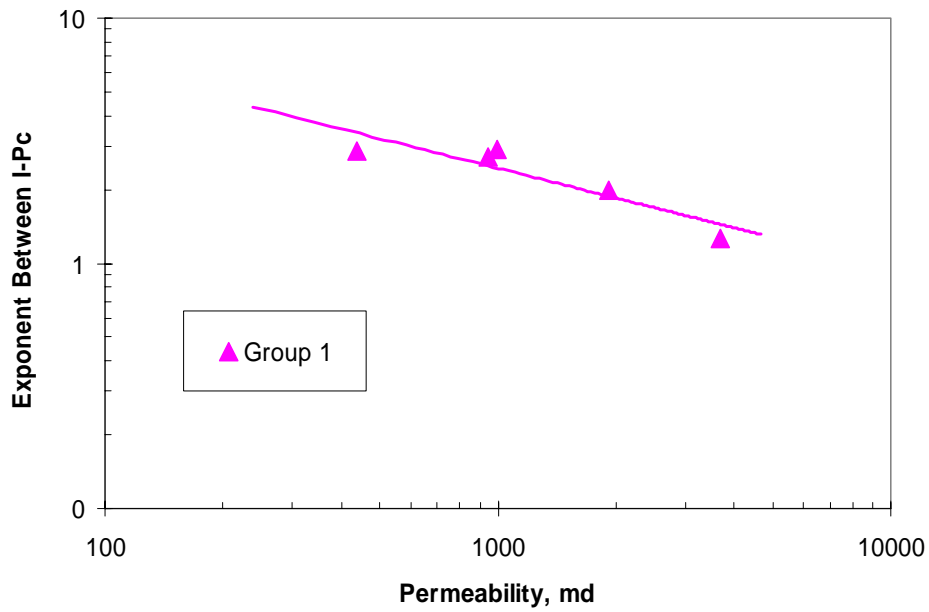


**Fig. 11: Effect of permeability on  $\beta$  for the core samples in Group 1 (high permeability)**

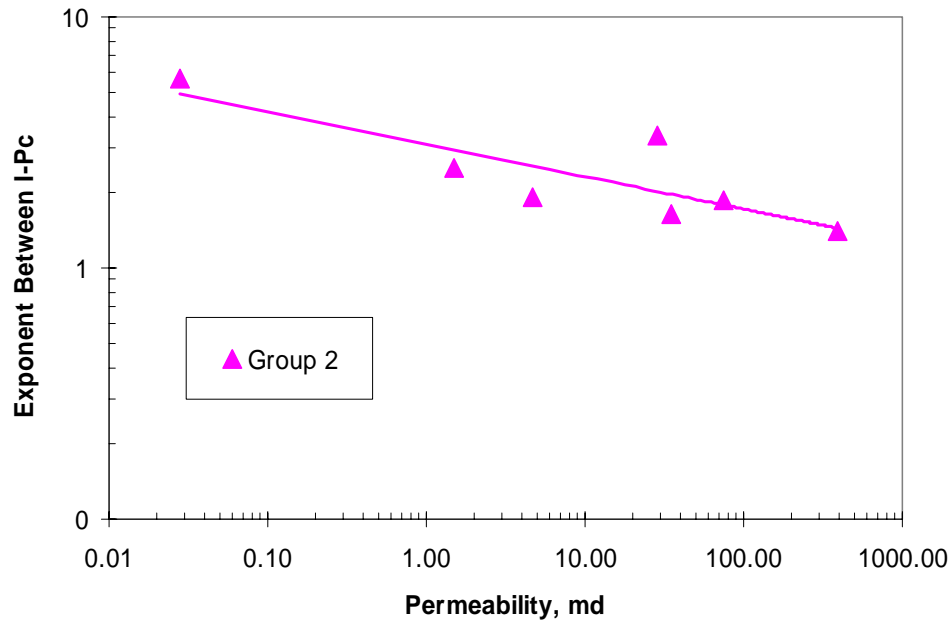


**Fig. 12: Effect of permeability on  $\beta$  for the core samples in Group 2 (low permeability)**

In the cases studied, for both Group 1 and 2, the value of  $\beta$  decreases with the increase in permeability. The relationship between permeability and  $\beta$  is linear in a log-log plot, as shown in Figs. 11 and 12. The values of correlation coefficient for Group 1 and 2 are 0.82 and 0.71 respectively.

## Discussion

As demonstrated in Fig. 7, the power law model proposed in this study to correlate capillary pressure and resistivity works properly for high values of capillary pressure and resistivity (corresponding to low values of water saturations). At high water saturations, the experimental data deviate the power law model. The possible reason may be that the distribution of water saturation may not be a fractal at high water saturations. This was also pointed out by Toledo *et al*<sup>4</sup>. Note that Eqs. 2 and 3 are only suitable for a specific range of water saturation with low values. In the case of low permeability core samples, the number of data points that deviate the power law model is less. This may be due to the fractal property of low permeability core samples. However this is yet to study in more detail.

Note that the linear model (Eq. 1) proposed by Szabo<sup>2</sup> can fit some experimental data for the high values of capillary pressure, especially in low permeability core samples. However the data point that fit the model are very few.

## Conclusions

The following conclusions may be drawn from the present study:

1. A model was developed theoretically to correlate capillary pressure and resistivity index. This model predicts a power law relationship between capillary pressure and resistivity index.
2. The model derived in this study was tested against experimental data in 14 core samples from an oil reservoir. The permeability ranged from 0.028 to over 3000 md. The results demonstrated that the model work satisfactorily.
3. The model works better in core samples with low permeabilities than those with high permeabilities.
4. The experimental results showed that the relationship between capillary pressure and resistivity index is not linear, as the existing model foresees.
5. The value of  $\beta$  decreases with the increase in permeability. The relationship between permeability and  $\beta$  is linear in a log-log plot in the cases studied.

## Acknowledgments

This research was conducted with financial support from the US Department of Energy under grant DE-FG07-02ID14418, the contribution of which is gratefully acknowledged. The authors thank CoreLab for the permission to publish these results.

## References

1. Li, K. and Horne, R.N.: "A Semianalytical Method to Calculate Relative Permeability from Resistivity Well Logs," SPE 95575, the 2005 SPE Annual Technical Conference and Exhibition, Dallas, TX, USA, October 9-12, 2005.
2. Szabo, M.T.: "New Methods for Measuring Imbibition Capillary Pressure and Electrical Resistivity Curves by Centrifuge," *SPEJ* (June, 1974), 243-252.
3. Longeron, D.G., Argaud, M.J., and Bouvier, L.: "Resistivity Index and Capillary Pressure Measurements under Reservoir Conditions using Crude Oil," SPE 19589, presented at the 1989 SPE Annual Technical Conference and Exhibition, San Antonio, TX, USA, October 8-11, 1989.
4. Toledo, G.T., Novy, R.A., Davis, H.T. and Scriven, L.E.: "Capillary Pressure, Water Relative Permeability, Electrical Conductivity and Capillary Dispersion Coefficient of Fractal Porous Media at Low Wetting Phase Saturation," SPE Advanced Technology Series (SPE23675), 2(1), 136-141, 1994.
5. Archie, G.E.: "The Electrical Resistivity Log as an Aid in Determining Some Reservoir Characteristics," *AIME Petroleum Tech.* (1942), 1-8.

**Table 1: Properties of Core Sample**

	Core No.	$\phi$ (f)	k (md)	$\rho_g$	F	$S_{wr}$ (f)	m	n	R
Group 1	1	0.272	941	2.66	10.4	0.112	1.80	1.87	0.99
	3	0.281	1192	2.66	8.41	0.116	1.68	1.86	0.99
	6	0.191	999	2.65	15.5	0.134	1.65	1.82	0.91
	8	0.227	3680	2.65	11.8	0.067	1.67	2.00	0.98
	10	0.321	437	2.65	8.00	0.167	1.83	2.11	0.96
	16	0.262	1916	2.66	9.27	0.078	1.66	1.97	0.95
Group 2	152	0.114	1.49	2.63	122.3	0.519	2.21	2.49	0.92
	153	0.077	0.028	2.64	380.9	0.796	2.32	2.39	0.98
	204	0.179	0.560	2.69	43.9	0.617	2.20	1.82	0.92
	299	0.185	4.63	2.66	40.4	0.446	2.19	2.13	0.98
	334	0.234	387.	2.65	18.5	0.222	2.00	2.02	0.98
	336	0.163	35.3	2.66	40.1	0.388	2.03	2.23	0.95
	418	0.211	74.0	2.70	26.0	0.454	2.09	2.26	0.99
	479	0.210	28.3	2.68	29.9	0.560	2.18	1.91	0.98